Nanoscale

PAPER

View Article Online
View Journal | View Issue

Cite this: *Nanoscale*, 2025, **17**, 15338

Passive nanorheological tool to characterise hydrogels

Moira Lorenzo Lopez, *[a,b] Victoria R. Kearns, [b] Eann A. Patterson[a] and Judith M. Curran[a]

Hydrogels are highly versatile, multi-phase materials with a wide variety of applications, due to their complex structures and tuneable features at the micron and sub-micron scale. Physical and chemical properties within the local environments contribute to the overall properties of a hydrogel. Current quantitative techniques used to characterise the properties of a hydrogel usually focus on bulk properties and are limited to identifying macroscopic properties, providing little information about local variations and heterogeneity, or fail to provide insight into real-time dynamic responses to external stimuli. These issues are especially challenging when characterising soft hydrogels due to their high-water content, which induces weak signals and noisy data. Here, we present a passive nanorheological tool that indirectly enables the characterisation of soft hydrogels at the micro/nanoscale by tracking nanoprobes with a label-free optical microscopy technique, making this an inexpensive, time-efficient, and user-friendly tool. This tool allows effective mapping of the properties in local micro/nano environments in heterogeneous soft materials thus permitting the identification of real-time sol–gel phase transition in thermosensitive hydrogels. Hence, this novel nanorheological characterisation tool has great potential for use in soft material design, manufacturing and quality control processes.

Received 27th February 2025,
Accepted 5th June 2025

DOI: 10.1039/d5nr00875a

rsc.li/nanoscale

Introduction

Hydrogels can be designed and engineered to present specific desired features, such as stiffness or mesh size, thus making them useful in a wide range of fields from biomaterials to electronics. They have applications in tissue engineering, drug delivery, water treatment, wearable technologies, and supercapacitors.[1–3]

Understanding a hydrogel's properties is crucial for meeting application-specific requirements, optimising performance, and designing novel materials. Thus, numerous methodologies have been developed to understand their mechanical and structural features. However, the characterisation of multi-phase hydrogels has posed several challenges linked to the intrinsic features that make them so versatile. The high water content and the low polymeric ratio have led to noisy data and weak signals in morphological characterisation techniques such as small-angle-scattering (SAXS) or scanning electron microscopy (SEM). Even refined techniques such as cryo-SEM, involving a fast freezing process of the sample, are linked to a change in the original materials' morphology.[4,5] Mechanical characterisation techniques usually rely on average values or bulk characterisation, such as rheology or tensile testing. For instance, their heterogeneous rheological behaviour at the micro/nanoscale might significantly differ from the single value provided by a bulk rheological measurement.[6] More localised tools, such as atomic force microscopy (AFM) or nanoindentation, are limited to surface indicators for the sample and are inapplicable for soft hydrogels.[7,8] Taking into consideration that the properties of soft materials at the micro and nanoscale are crucial for understanding and their use in many biological and physical phenomena, such as cell differentiation or electrical conductivity, their enhanced characterisation in real-time is needed.[9,10]

Microrheology has emerged as a tool to provide viscoelastic properties of soft materials with a high spatial resolution.[11] This technique includes both active microrheology, based on the application of an external force such as magnetic, centrifugal, or gravitational, and passive microrheology. The fundamentals of passive microrheology were first described by Mason and Weitz's work in 1995 who employed probes, dispersed colloidal particles in this case at the micrometre scale (1–100 μm), where temperature-induced molecular motion causes particles to experience Brownian motion.[12] The random motion of a particle can be characterised by its mean-squared displacement (MSD) from a reference position which is directly proportional to the time interval over which the MSD is measured and the diffusion constant, D. The

[a]School of Engineering, University of Liverpool, Liverpool L69 3BX, UK.
E-mail: M.Lorenzo-Lopez@liverpool.ac.uk
[b]Department of Eye and Vision Science, University of Liverpool, Liverpool L7 8TX, UK

Stokes–Einstein relationship defines the diffusion coefficient, D of single particles of known radius, r in a fluid at a set temperature, T as follows:[13]

$$D = \frac{k_b T}{6\pi\eta r} \quad (1)$$

where k_b is the Boltzmann constant, and η is the fluid viscosity. Hence, an experimental determination of the diffusion constant based on the MSD of a particle allows the viscosity of the fluid to be evaluated.

This concept has been extended to passive nanorheology using probes at the nanometre scale (nanoprobes) monitored with diffusing wave spectroscopy, laser deflection particle tracking or other laser interoferometric methods to calculate the viscoelastic properties of the media in which the probes are diffusing, including both viscosity and the complex shear modulus.[14,15] The smaller size of nanoprobes provides insights into the mechanical properties of complex materials within a more confined environment and at increasing resolution.[15] However, some inconsistencies have been observed in different experimental setups, including entangled polymer melts and molecularly-thin films, for which it has been acknowledged that the classical Stokes–Einstein relationship is not relevant.[14,16] These nanorheology techniques are based on the generalised Stokes–Einstein (SE) equation, in which the diffusion of particles is inversely proportional to the viscosity of the media, as stated above in eqn (1).[17] However, this relationship is based upon several assumptions, including a constant value of hydrodynamic diameter, the shape of the particle being spherical, and the continuum hypothesis, which states that the diffusing particle experiences the medium as a continuum and assuming macroscopic hydrodynamics.[18]

Previously reported data has demonstrated the decreasing reliability of the classical Stokes–Einstein relationship when the scale approaches the molecular level.[18] Measurements have shown that there is a critical particle diameter below which the classical Stokes–Einstein relationship is invalid and overpredicted the diffusion coefficient.[19,20] The critical particle diameter was found to be in the range 150–300 nm depending on the viscosity of the media and concentration of the nanoparticles.[21] For that reason, the use of the classical Stokes–Einstein relationship to obtain viscoelastic parameters from experimental values of diffusion is not appropriate; and, instead, the fractional Stokes–Einstein relationship should be used. In the fractional Stokes–Einstein relationship, diffusion is independent of particle size and inversely proportional to viscosity in the logarithmic domain, *i.e.*, there is linear relationship between $\log D$ and $\log \eta$, as shown previously.[21]

Here, we present a novel passive nanorheological tool, which indirectly characterises the localised rheological properties of phases of hydrogels through the correlation of nanoparticle motion and the environment they are diffusing in, at the nanoscale and in real-time, using the fractional Stokes–Einstein relationship. The nanoparticle motion is assessed with a label-free microscopy platform based on the optical phenomena of caustics, a natural phenomenon generated by the refraction of the light when it encounters a curved surface, creating envelopes of light and shadows. When this is applied in an optical inverted microscope, by increasing the coherence of the light, the nanoparticles are visualised as black and white concentric circles (caustics), permitting their visualisation and tracking over time in a label-free manner as shown in the schematic in Fig. 1.[22]

First, we experimentally validate nanoprobes' diffusive values in simple Newtonian fluids with their empirical viscosity to create a standard tool using this microscopy platform. This tool was then used to help understand the viscous properties of localised environments within heterogeneous agar–hyaluronic acid hydrogels through the motion of nanoparticles. Second, to assess the dynamic response to stimuli of hydrogels in real-time, we expanded the capabilities of this tool to characterise the volume phase transition temperature in a well-characterised, thermosensitive hydrogel.

Results and discussion

To overcome current limitations in the characterisation of soft-materials properties at the micro/nanoscale in real time, a non-destructive passive nanorheological platform has been developed, as an inexpensive and user-friendly solution, and tested it in a range of hydrogels that have been extensively used in biological applications.

Firstly, the validation of the passive nanorheological platform was performed with the use of simple and Newtonian fluids. For that, different glycerol solutions in deionized water DIW (v/v) and silicone oil were used to obtain a wide range of viscosity values, ranging from 0.001 to 5 Pa s, as shown in Table 1. 100 nm citrate-capped gold nanoparticles were selected as nanoprobes due to their well-established characterisation and their near-neutral surface charge, which was important to avoid interactions with charged hydrogels.[23] Their motion was tracked using the label-free nanoparticle tracking technique in the optical inverted microscope (Fig. 1). The bulk values of viscosity for each media, measured using the compact rheometer, were correlated with the measured values of the diffusion coefficient of the 100 nm nanoprobes in each environment.

A strong linear negative relationship was obtained between the logarithm of the experimental values of diffusion coefficient ($D_{100\ nm}$) and the logarithm of the viscosity of the media (η) with a correlation coefficient of 0.99, shown in Fig. 2. This validates the relationship between these two quantities and enables the motion of the gold nanoprobes to be used as a comparable rheological dynamic analysis model for the viscosity of the medium. Mathematically, this relationship can be expressed, using the fractional Stokes–Einstein relationship, as:

$$\log(D_{100\ nm}) = -0.87\log(\eta) - 14.35 \quad (2)$$

Secondly, to map the intrinsic heterogeneity of hydrogels, 100 nm nanoprobes were dispersed, at low concentrations, in

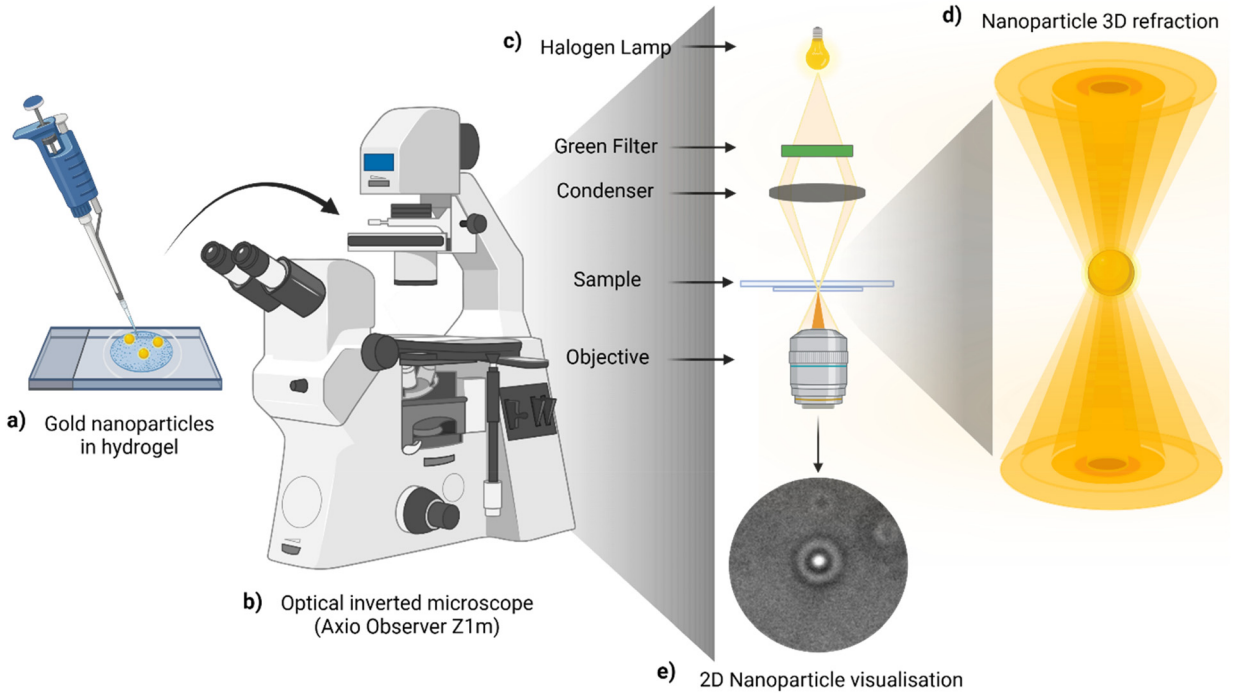

Fig. 1 Schematic diagram of the nanoparticle label-free tracking technique based on optical microscopy. (a) A small aliquot of the sample (~50 μL) is introduced in the microscope slide cavity; (b) the sample is visualised under an inverted optical microscope (Axio Observer Z1.m); (c) the coherence of the light is increased by the addition of a green filter in the light pathway, by closing the condenser to the minimum and by setting the microscope to Kohler illumination; (d) when the light hits the nanoparticles this creates a diffraction pattern in 3D; (e) in 2D this is shown as black and white (light and shadows) concentric circles, bigger than the actual nanoparticle making it visible and trackable over time. Figure created with BioRender.

heterogeneous agar–hyaluronic acid hydrogels: low viscous (LV), medium viscous (MV) and high viscous (HV). Preliminary qualitative evaluations showed that there was a correlation between the characterised movement of the nanoparticles in a local area and the material properties/phase associated with that area. This can be seen in Fig. 3, where nanoparticles associated with a more aqueous-based phase were found to move further away from their starting point (Fig. 3a), others were found to be 'dancing on the spot' (Fig. 3c) in a more polymeric phase, and some presented an intermediate behaviour corresponding to a transition phase (Fig. 3b).

Table 1 Simple Newtonian fluids used to validate the passive nanorheological platform. The specified media was used at different temperatures to obtain the set range of viscosity values

MEDIA	Temperature (°C)	Viscosity (Pa s)
Deionised water (DIW)	20	0.001
55% glycerol in DIW (v/v)	37	0.005
75% glycerol in DIW (v/v)	20	0.05
90% glycerol in DIW (v/v)	34	0.1
100% glycerol	30	0.42
100% glycerol	20	1
Silicone oil (Siluron® 5000)	25	5

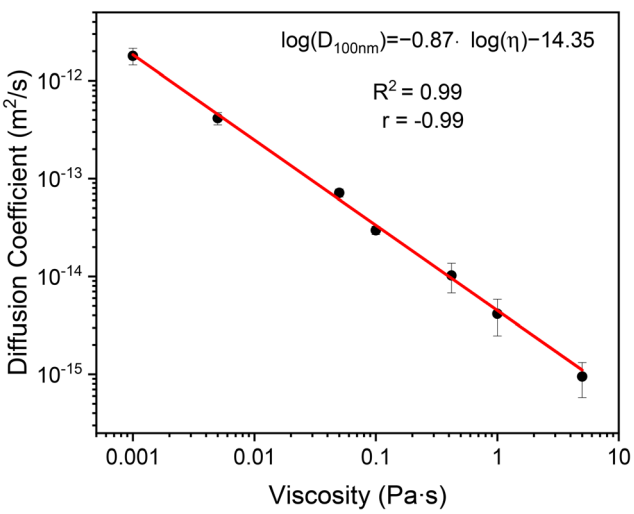

Fig. 2 Diffusion coefficient of nanoprobes (100 nm gold nanoparticles) plotted as a logarithmic function of viscosity of the simple-homogeneous media (glycerol solutions and silicone oil) they are diffusing in. The black dots represent the mean values of 10 nanoprobes' diffusion coefficients, and the error bars state the standard deviation. The high value of R^2 = 0.99 shows the usefulness of the set equation to extrapolate viscosity values to define the environment where the nanoprobes are diffusing.

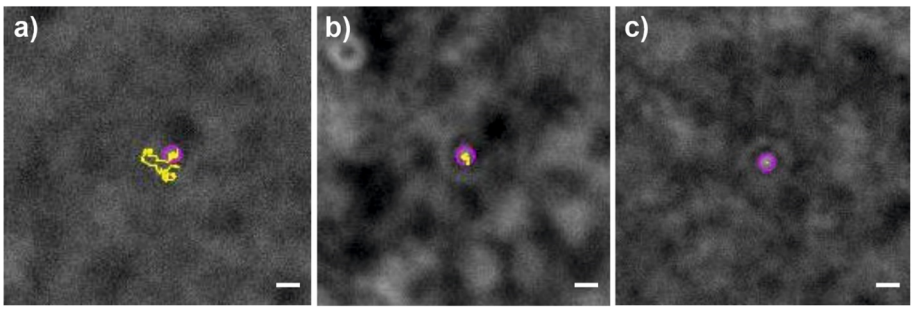

Fig. 3 Path of motion, or tracks over a 100 frames (2.5 seconds) of 100 nm nanoprobes diffusing in the medium viscous agar hyaluronic acid hydrogel revealing the heterogeneity of this hydrogel where (a) some nanoparticles diffused in an aqueous environment with longer paths; (b) some nanoparticles were found to have a more restricted movement in an intermediate/transition phase; and (c) some nanoparticles moved around a spot and were believed to be interacting with the gel phase.

To assess the viscosity values of each localised environment, thirty random nanoprobes were analysed in each hydrogel, maximising the dispersion of the nanoprobes across the different localised environments, while maintaining a good time efficiency ratio. The experimental values of diffusion coefficients of these tracked nanoparticles are presented in Fig. 4 as a function of the bulk viscosity of the hydrogels fitted to the Carreau–Yasuda model.[24]

The presence of multiple diffusion values for a sole hydrogel shows the inaccuracy of a single bulk value in describing the mechanical properties of these hydrogels and characterises localised environments that can be associated with distinct phases. Diffusion values above 10^{-13} m^2 s^{-1} align with an aqueous-base phase, under 10^{-14} m^2 s^{-1} will characterise a gel-phase, and between both we can find nanoprobes in a transition phase; in agreement with previously reported data.[25] Using eqn (2), specific viscosity values can be extracted for the different localised environments in which each nanoprobe diffuses. The low viscous (LV) and medium viscous (MV) hydrogels showed a wide range of viscosity values ranging from near water with 0.001 and 0.002 Pa s for LV and MV, respectively, to values in the range of high viscous silicone oils ≈5 Pa s. The high viscous hydrogel (HV) presented a wide range of high viscosities, with values ranging from 2 Pa s to ≈40 Pa s, which is consistent with the higher polymer (agar)

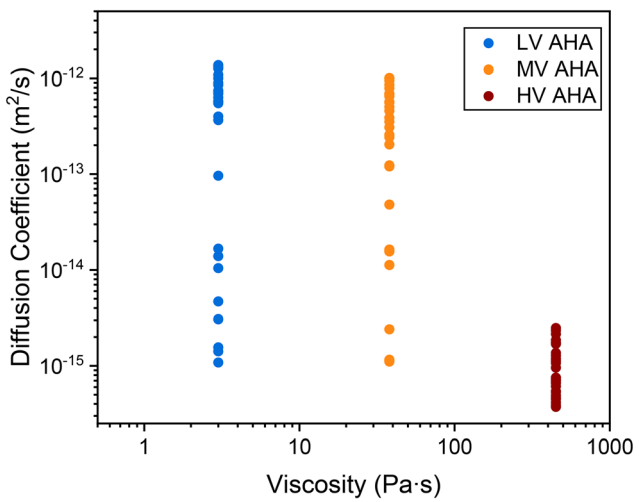

Fig. 4 Distribution of diffusion coefficient values of 100 nm gold nanoprobes in the three agar–hyaluronic acid hydrogels (AHA) with low (LV-blue), medium (MV-orange), and high (HV-red) viscosity. The wide distribution of diffusion coefficients for single bulk values of viscosity shows the limitations of macrorheology and the distribution of localised environments within the hydrogels at the micro/nano scale. Where values of diffusion above 10^{-13} m^2 s^{-1} characterise an aqueous phase, values under 10^{-14} m^2 s^{-1} a gel phase, and those in between are categorised to be in an intermediate/transition phase.[25]

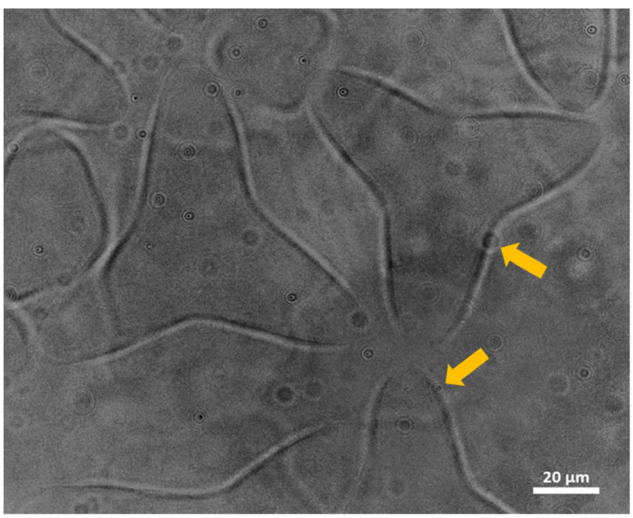

Fig. 5 Pluronic® F127 20% with 100 nm gold nanoprobes during the heterogeneous transition from soluble to gel phases induced by a temperature ramp from 20 °C to 40 °C, visualised under an inverted optical microscope adjusted for caustics. The label-free visualisation enables the characterisation of the different environments that are created during the sol–gel transition. Some nanoprobes are found in the sol phase and others in the gel phase; moreover, the limit of these two phases can be determined through the visualisation of nanoprobes in the interface between phases (yellow arrows). This image was taken at mid-sample, ~100 µm from the bottom of the sample.

concentration and probably characterising different levels of crosslinking in different regions of the gel.

Finally, to assess the hydrogel's dynamic response to an external stimulus in real time, we used Pluronic® F127, a widely studied thermosensitive hydrogel.[26] Pluronic® F127 is a tri-block copolymer that has become a promising hydrogel facilitating the encapsulation and release of water-insoluble and water-soluble drugs through the formation of polymeric micelles. Its formulation at 20% (w/v) has been reported to exhibit this behaviour and transition to gel at near body temperatures (37 °C), making it a good fit for different drug delivery applications, such as ophthalmic formulations and wound healing therapy, by facilitating their injection in the sol state.[27,28] Experiments were conducted in the inverted optical microscope set-up for viewing caustics and with a temperature-controlled stage. The Pluronic® F127 was seeded with gold nanoprobes and the stage temperature raised from 20 °C to 40 °C inducing a sol-to-gel transition. The experiments uncovered, on one hand, the near-homogenous nature of Pluronic® in both the sol and the gel state when these were temperature-stabilised; and, on the other hand, an heterogenous complexion when the polymer was in the phase transition state (Fig. 5). Moreover, we found that this dynamic process can be characterised through the presence of nanoprobes, where their distribution throughout the sample permits the characterisation not only of the sol and gel phases but the interface between them through the presence of nanoprobes at the sol–gel boundaries (seen by yellow arrows in Fig. 5).

The sol-to-gel transition creates a difference in viscosity within the sample in response to the temperature increase; making this a heterogeneous state where both phases (sol and gel) coexist, shown in Fig. 5 and 6. The difference in heat distribution creates difference in the gel-forming patterns where,

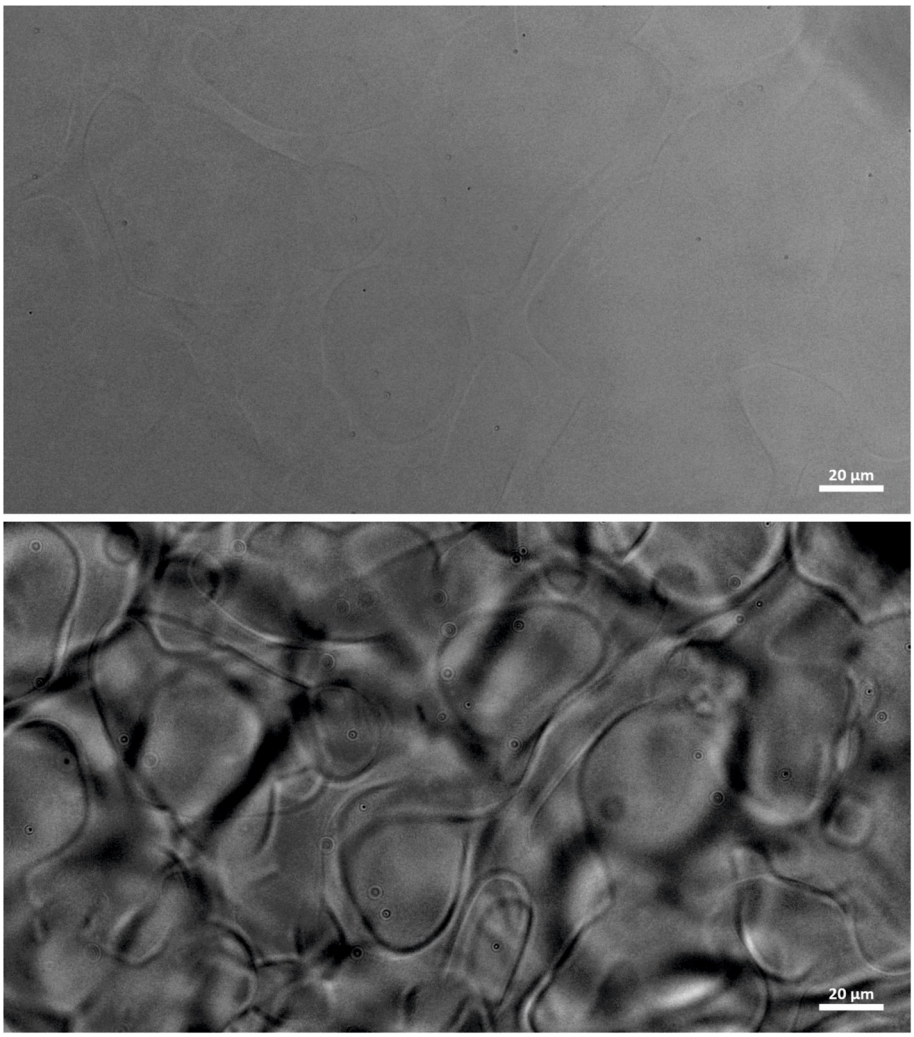

Fig. 6 Microscope images of Pluronic® F127 20% with gold nanoparticles at 28 °C during the sol–gel transition. The top image shows the transition with the microscope set to normal bright field conditions, and the bottom image shows the high level of detail that is created when the microscope is set-up for the optical phenomena of caustics. These images were taken at ~25 μm from the bottom of the sample.

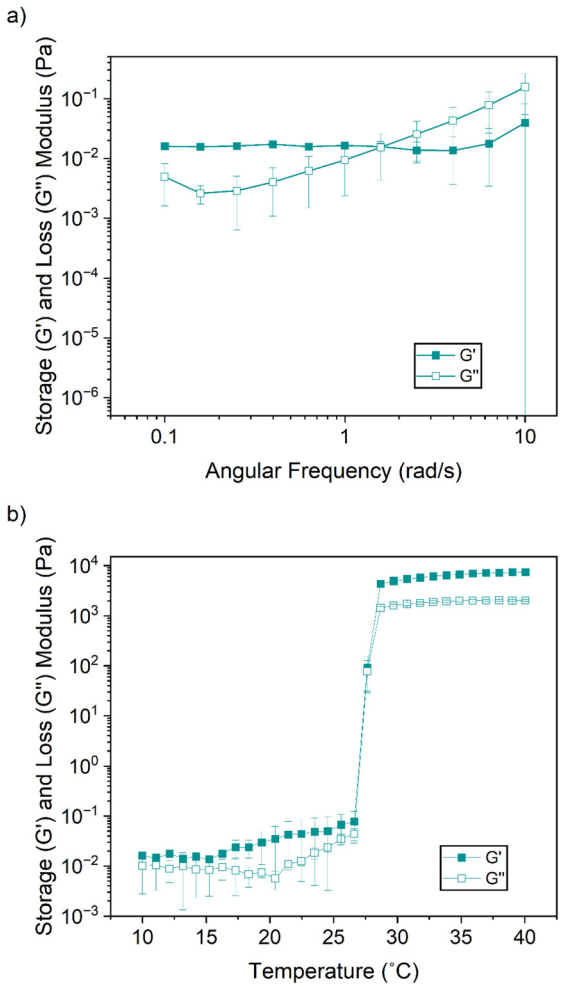

Fig. 7 Rheological characterisation of Pluronic® F127 20%, values shown are a mean of one test from 3 different formulations and error bars represent the standard deviation; for (a) frequency sweep showing a linear viscoelastic region from 0.1 to 1 rad s^{-1} and (b) temperature ramp from 10 °C to 40 °C, with a steep phase transition from sol-to-gel occurring at 28 °C, beyond which more stable values of *G*′ and *G*′′ show a clear viscoelastic behaviour where elastic properties dominate, indicating a gel-like state.

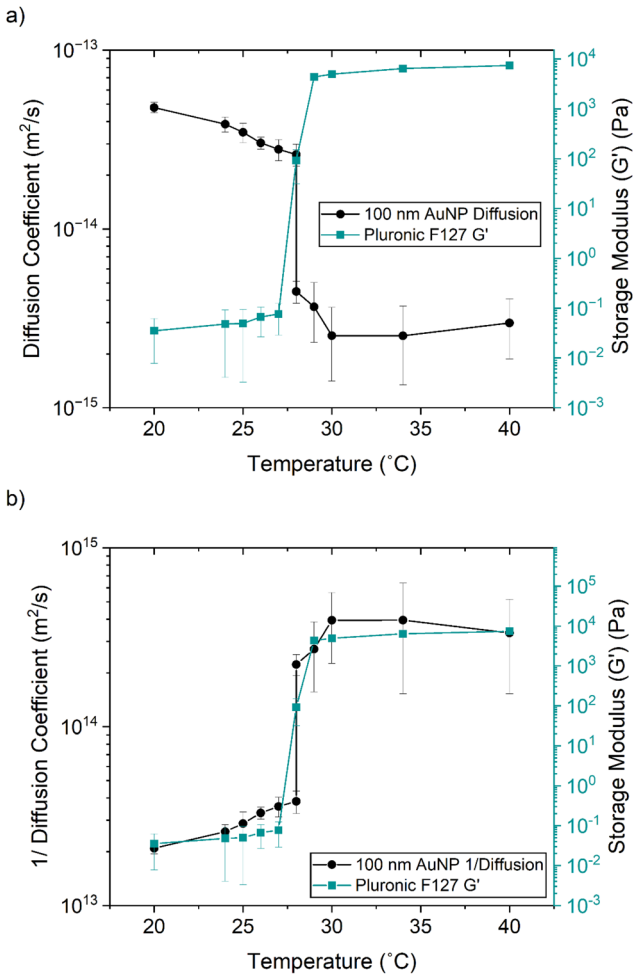

Fig. 8 Phase transition temperature of Pluronic® F127 20% shown using the storage modulus, *G*′ (turquoise squares) and the diffusion coefficient, *D* for 100 nm nanoprobes (black circles) showing that both methods indicate the same transition temperature of 28 °C. (a) Low values of *G*′ correlate with high values of diffusion, characterising an aqueous phase, and high values of *G*′ correlate with low values of nanoparticles' diffusion, characterising the gel phase. Moreover, at 28 °C, the nanoparticles showed a dual behaviour, with both fast and slow diffusing particles, characterising this transition as heterogeneous, where both phases coexist. (b) The representation of nanoprobes' inverse diffusion coefficient values shows clearer the inverse relationship between nanoprobes motion and the rheological properties of the media they are in.

at mid sample height (~100 μm) the patterns were more consistent in shape and size (Fig. 5) and closer to the bottom of the sample (~25 μm) these were found to resemble Rayleigh–Bènard convection cells, shown in Fig. 6.[29]

The specific bulk phase transition temperature was assessed through a rheology temperature ramp (10 °C to 40 °C). In the compact rheometer, a first frequency sweep identified the linear viscoelastic range of Pluronic® to be from 0.1 to 1 rad s^{-1} (Fig. 7a). The optimised frequency at 0.3 rad s^{-1} was selected for the temperature ramp, which showed a steep phase transition at 28 °C (Fig. 7b), after which a viscoelastic behaviour dominated by the elastic domain (*G*′) characterises the stable gel formation, in agreement with previous Pluronic® bulk rheological characterisation.[30]

The potential of the nanorheological tool to precisely characterise the phase transition temperature was assessed by quantifying the diffusion of 100 nm nanoprobes at different specified temperatures from 20 °C to 40 °C. At low temperatures (<28 °C) low values of *G*′ (turquoise squares in Fig. 8a), showing a sol state of the Pluronic® F127, correspond with high values of diffusion (>2 × 10^{-14} m^2 s^{-1}) (black circles in Fig. 8a) of the nanoprobes. At the same time, high temperatures (>28 °C) show high values of *G*′ corresponding with a gel state of the Pluronic® where the nanoprobes were found stranded in the matrix, presenting low values of diffusion (in the range of 10^{-15} m^2 s^{-1}). More interestingly, at 28 °C in agreement with the bulk rheological characterisation of the phase transition temperature, nanoprobes were found to

present a dual behaviour, where some were still diffusing in the sol phase ($\sim 10^{-14}$ m^2 s^{-1}), and others were already diffusing in the gel phase, presenting values of diffusion in the other of 10^{-15} m^2 s^{-1}, as shown in Fig. 8. This also agrees with the qualitative characterisation of this phase transition point as an heterogenous state where both phases coexist, as shown in Fig. 5 and 6. The inverse representation of the nanoprobe's diffusion values, in Fig. 8b, shows the phase transition in the same format as the bulk characterisation using the storage modulus (G').

Overall, the data presented demonstrates that the characterisation of nanoprobes' motion provides an accurate reflection of the local time dependent features at a micro/nanoscale of low-viscous hydrogels, including the localised viscosity values in heterogeneous soft materials and the real-time sol-to-gel phase transition for thermosensitive hydrogels.

This mechanical characterisation of hydrogels is essential, for instance, in biomaterials, where their main applications are as biomimetics, scaffolds for tissue regeneration and drug delivery.[26,31,32] Complementary to macrorheological analysis, the understanding of these properties at the micro/nanoscale is of especial importance in these mentioned applications as the micro/nano environment will define cell fate, toxicity, and injectability.[33,34] Thus, passive micro/nanorheology tools can enhance the understanding and the ability to replicate such desired biological features.[35] Moreover, passive nanorheological analysis are also better suited for the characterisation of soft hydrogels with low moduli values, usually used in biomaterials, when compared to active nanorheological tools.[11]

This non-destructive passive nanorheological tool holds the potential to eliminate some of the challenges to characterising hydrogels (shown in Table 2) by its incorporation in the design and manufacturing processes for soft materials. This tool enables the mapping of the spatial-rheological heterogeneity in the material's native state using a standard inverted microscope with a small volume sample (~50 μL) and minimal to no sample preparation. Moreover, this measurement technique shows promise for use in product quality control processes, including degradability and stability assays of many hydrogels through the characterisation of their phase transition or analysis of their microstructure stability in real time.

In addition, this platform holds the potential to be used for many not opaque materials including other soft materials such as colloidal suspensions or microgels, and epoxy-based polymers. The technique may allow the characterisation of their phase transition at the micro/nano-level in response to different external factors such as magnetic, thermal, or electric stimuli.[36–38] However, additional experiments would be necessary to verify these potential applications.

Experimental

Glycerol solutions

99% pure glycerol was purchased from Fisher Scientific (UK) and used to increase the viscosity of the diffusive media

Table 2 Comparison of different hydrogel mechanical characterisation techniques. (AFM = Atomic Force Microscopy)

	Technique	Resolution	Sample preparation	Depth of characterisation	Required expertise	Limitations	Advantages	Ref.
Uniaxial testing	Bulk rheology Compression	Macroscale Macroscale	Minimal Cylindrical/disc samples	Bulk properties Bulk properties	Moderate Moderate	Characterises bulk properties of the material.	Fast and requires small sample sizes (~1 g)	41 and 42
	Tensile	Macroscale	Strip shape sample (high stiffness)	Bulk properties	Moderate	Inconvenient for soft materials, not easy to hold hydrogels.		43
Microrheology	Active (optical tweezers/magnetic fields)	Microscale	External stimuli needed (magnetic probes when appropriate)	Local properties through entire sample	High	Requires application of external forces, time consuming and prior information of the material required.	Convenient for stiffer materials and potential nonlinear microrheological measurements.	44 and 45
	Passive	Microscale	Minimal	Local properties through entire sample	Low-Moderate	Microparticles might be larger than the materials' structure.	Convenient in soft materials with low moduli/viscosity.	11 and 35
Nanorheology	Active (AFM/ nanoindentation)	Nanoscale	Flat, clean, thin	Local surface properties	High	High cost and needs strong moduli/viscosity materials.	AFM permits the creation of a topographic map of the materials' surface.	46
	Passive conventional techniques	Nanoscale	Particle staining	Local properties through entire sample	High	Based on Stokes–Einstein equation and needs sample staining.	Informs of local viscoelasticity at the submicron scale.	14 and 15
	Novel proposed passive technique	Nanoscale	Minimal	Local properties through entire sample	Low	Use of soft materials that allow the light to pass through.	User friendly, fast, low cost and small sample size (~50 μL).	25 and 47

through different solutions in deionised water (DIW) of 0, 55, 75, 90 and 100% glycerol (v/v).

Silicone oil

Highly purified silicone oil (Siluron® 5000) was donated by Fluoron GmbH (DE) and used as received.

Agar–hyaluronic acid hydrogel synthesis

Agar–hyaluronic acid (AHA) hydrogels were synthesised following the protocol described by Thakur *et al.*[39] Three hydrogels with different viscosities were synthesised by adding different concentrations of agar (Sigma-Aldrich, UK) and hyaluronic acid (high molecular weight) (cosmetic grade, Amazon, UK) to 1× boiling phosphate buffered saline (PBS) (Gibco, UK). To create a high viscous (HV) hydrogel, hyaluronic acid was used at a concentration of 5 mg mL^{-1} and agar at 4 mg mL^{-1}; for a medium viscous (MV) hydrogel, the concentrations of hyaluronic acid and agar were 2.21 mg mL^{-1} 1.8 mg mL^{-1} respectively; and for a low viscous (LV) hydrogel, the corresponding concentrations were 0.7 mg mL^{-1} and 0.95 mg mL^{-1}. The solutions were magnetically stirred at 100 °C for 1 hour, after which the gels were cooled down to room temperature overnight before being used in characterisation experiments.

Pluronic® F127 hydrogel synthesis

20% (w/v) Pluronic® F127 (Sigma-Aldrich) was prepared by dissolving the polymer in a solid state in DIW through magnetic stirring at a temperature below 6 °C. Solutions were left overnight in the fridge (<6 °C) before rheological characterisation.

Standard bulk rheology

An Anton Paar Modular Compact Rheometer (MCR 302) with a stationary lower plate was used to make rheological measurements. A viscosity shear rate sweep was performed to obtain experimental viscosity values of the glycerol solutions and silicone oil. This was performed with a parallel plate 40 mm in diameter and a shear rate range of 0.1 to 300 s^{-1}. The rheological characterisation of the hydrogels was done using a parallel measuring geometry 40 mm in diameter with a rough surface to avoid wall slip and ensure adhesion of the sample to the geometry. A solvent trap was used to eliminate solvent loss during the analysis of the samples by creating a thermally stable vapour barrier.

To characterise the static bulk viscosity values of the agar–hyaluronic acid hydrogels, a viscosity shear sweep at 34 °C was performed, ranging from 0.01 to 100 s^{-1}. The results were fitted to the Carreau–Yasuda model.[24]

Pluronic® F127 was first analysed with a frequency sweep as a mean of three tests. These sweeps were performed to identify the linear viscoelastic region at a constant strain of 0.5% for 0.01 to 100 rad s^{-1}. The optimised strain (0.5%) and frequency (0.3 rad s^{-1}) values were used to perform a temperature ramp from 10 °C to 40 °C, with a constant heating rate of 0.5 °C min^{-1}, to characterise its phase transition temperature.

Novel localised rheology

Gold nanoparticles of 100 nm in diameter (spherical citrate capped from BBI Solutions, UK) were added to the glycerol solutions and to the hydrogels to reach a concentration of 10^{-4} mg mL^{-1}. It should be noted that for the suspension of nanoparticles in the hydrophobic silicone oil, the buffer was evaporated to leave dry nanoparticles. The 10 μL of the citrate-capped nanoparticles stock solution was added into a 5 mL bottle; this was left to evaporate in a cell culture hood overnight. Once evaporated, 1000 μL of silicone oil (to reach a concentration of 10^{-4} mg mL^{-1}) was added and the solution was let to stir for 72 hours. Prior to nanoparticle tracking, the silicone oil suspension was left to stabilise for 24 hours.

The samples were vortexed and sonicated for 1 minute before being aliquoted (50 μL) into a single cavity microscope slide (76 × 26 mm and 150 μm cavity depth). The label-free visualization and tracking of nanoparticles was done in an Axio Observer.Z1 m (Carl Zeiss, DE) inverted optical microscope. The incorporation of a green interference filter (Olympus, JP, centred on 550 nm, 45 nm bandwidth), the closure of the condenser to the minimum (1 mm) and the setting to Köhler illumination increases the coherence of the light (source: halogen lamp) resulting in the nanoparticles creating caustic signatures (Fig. 1). The microscope was equipped with a stage-top incubation system (Incubator PM S1, Heating Insert P S1, Temp and CO_2 module S1, Carl Zeiss, DE), which was used to maintain the samples at the desired temperatures. Videos of randomly selected single nanoparticles were recorded for each media. In the simple Newtonian fluids (glycerol solutions and silicone oil) 10 particles were tracked; for the non-Newtonian hydrogels the number of particles was increased to ensure accuracy, 15 nanoparticles in the thermosensitive hydrogel (Pluronic® F127 20%) and the number were doubled (30) in the heterogeneous (agar–hyaluronic acid) hydrogels, to better understand their micro–nano environment. The tracking was performed from videos recorded using a ×40 objective and a monochromatic camera (Axiocam305, Carl Zeiss, DE) with a spatial resolution of 0.086 μm^2 for one pixel and a temporal resolution of 48 fps.

Phase temperature transition assay

100 nm gold nanoparticles were added to 20% (w/v) Pluronic® F127. The solution was vortexed for 30 seconds and sonicated for 1 minute prior to aliquoting 50 μL into a single cavity microscope slide. The sample was incubated in the temperature-controlled microscope stage for 10 minutes for each temperature of the following series of temperatures 20 °C, 24 °C, 25 °C, 26 °C, 27 °C, 28 °C, 29 °C, 30 °C, 37 °C, 40 °C to enable thermal stability in each condition. Videos of 15 randomly selected nanoparticles were recorded for each temperature condition.

Data analysis

The videos were processed using ImageJ software through the TrackMate plugin,[40] from where the X and Y positions of the

nanoparticles were obtained over time. Experimental values of diffusion coefficient were extracted from the mean squared displacement (MSD) relation (3), following the same procedure reported by Lorenzo *et al.*[25]

$$D = \frac{\mathrm{MSD}}{2d\Delta t} \quad (3)$$

where D is the experimental value of diffusion coefficient, MSD is the mean squared displacement, d is the number of dimensions of the system (in this case, 2), and Δt is the time lag.

Conclusion

A novel passive nanorheological measurement technique has been described and demonstrated to be useful in the characterisation of hydrogel properties, specifically localised viscosity, and of features, such as heterogeneity and phase transition at the micro–nano scale. Thus, significant challenges of current techniques, such as weak signals due to the high-water content and the dynamism of hydrogels, were overcome. The new technique is a time-efficient, user-friendly, and inexpensive way to empirically identify soft materials' features at the micro/nanoscale and has the capability to provide quantitative information in real-time on dynamic events. Hence, it has the potential to be useful in the design, synthesis, and quality control of hydrogels and potentially other soft materials such as microgels and epoxy-base polymers.

Author contributions

MLL performed data curation, analysis, and writing of first draft; VRK advised on hydrogels, EAP advised on data analysis and microscopy technique, JMC PI and grant holder. All authors contributed to manuscript writing and editing.

Data availability

The datasets generated and/or analysed during the current study are available in the repository [DataCat: The Research Data Catalogue] at **https://doi.org/10.17638/datacat.liverpool.ac.uk%2F2899**.

Conflicts of interest

There are no conflicts to declare.

Acknowledgements

This work was supported by the Doctoral Network in Technologies for Healthy Aging; and the Engineering and Physical Sciences Research Council [grant numbers EP/R024839/1; EP/S012265/1]. Silicone oil was provided to VK by Fluoron GmbH, Ulm, Germany. We would like to acknowledge Professor Rob Poole for facilitating his rheology laboratory, and Dr Anders Aufderhorst-Roberts for his insights in the rheological data.

References

1 M. Vigata, C. Meinert, D. W. Hutmacher and N. Bock, *Pharmaceutics*, 2020, **12**, 1–45.
2 Z. Zhang, H. Fu, Z. Li, J. Huang, Z. Xu, Y. Lai, X. Qian and S. Zhang, *Chem. Eng. J.*, 2022, **439**, DOI: **10.1016/j.cej.2022.135756**.
3 X. Cao, C. Jiang, N. Sun, D. Tan, Q. Li, S. Bi and J. Song, *J. Sci.:Adv. Mater. Devices*, 2021, **3**, 338–350.
4 D. McDowall, D. J. Adams and A. M. Seddon, *Soft Matter*, 2022, **8**, 1577–1590.
5 Z. Kaberova, E. Karpushkin, M. Nevoralová, M. Vetrík, M. Šlouf and M. Dušková-Smrcková, *Polymers*, 2020, **12**(3), DOI: **10.3390/polym12030578**.
6 T. De Maeseneer and R. Cardinaels, in *Injectable Hydrogels for 3D Bioprinting*, 2021, pp. 238–266.
7 B. R. Denzer, R. J. Kulchar, R. B. Huang and J. Patterson, *Gels*, 2021, **7**, DOI: **10.3390/gels7040158**.
8 P. Patel and P. Thareja, *Eur. Polym. J.*, 2022, **163**, 110935.
9 J. Yang, Y. Li, Y. Liu, D. Li, L. Zhang, Q. Wang, Y. Xiao and X. Zhang, *Acta Biomater.*, 2019, **91**, 159–172.
10 C. Zhou, T. Wu, X. Xie, G. Song, X. Ma, Q. Mu, Z. Huang, X. Liu, C. Sun and W. Xu, *Eur. Polym. J.*, 2022, **177**, DOI: **10.1016/j.eurpolymj.2022.111454**.
11 E. M. Furst and T. M. Squires, *Microrheology*, Oxford Academic, Oxford, 2017, ch. 3, pp. 86–132.
12 T. G. Mason and D. A. Weitz, *Phys. Rev. Lett.*, 1995, **74**, 1250–1253.
13 A. Einstein, Investigations on the Theory of the Brownian Movement, Translated by Dover publications, *Physics Bulletin*, 1956, vol. 7.
14 A. Mukhopadhyay and S. Granick, *Curr. Opin. Colloid Interface Sci.*, 2001, **6**, 423–429.
15 T. Ge, G. S. Grest and M. Rubinstein, *Phys. Rev. Lett.*, 2018, **120**(5), DOI: **10.1103/PhysRevLett.120.057801**.
16 T. Ge, *Macromolecules*, 2023, **56**, 3809–3837.
17 L. H. Cai, S. Panyukov and M. Rubinstein, *Macromolecules*, 2011, **44**, 7853–7863.
18 A. Tuteja, M. E. Mackay, S. Narayanan, S. Asokan and M. S. Wong, *Nano Lett.*, 2007, **7**, 1276–1281.
19 M. J. Solomon and Q. Lu, *Curr. Opin. Colloid Interface Sci.*, 2001, **6**, 430–437.
20 F. Giorgi, D. Coglitore, J. M. Curran, D. Gilliland, P. Macko, M. Whelan, A. Worth and E. A. Patterson, *Sci. Rep.*, 2019, **9**, 1–6.
21 D. Coglitore, S. P. Edwardson, P. Macko, E. A. Patterson and M. Whelan, *R. Soc. Open Sci.*, 2017, **4**(12), DOI: **10.1098/rsos.170507**.
22 E. A. Patterson and M. P. Whelan, *Nanotechnology*, 2008, **19**(10), DOI: **10.1088/0957-4484/19/10/105502**.

23 C. Louis and O. Pluchery, *Gold Nanoparticles for Physics, Chemistry and Biology*, 2nd edn, 2017.
24 T. Salahuddin, A. Javed, M. Khan, M. Awais and B. Al Alwan, *Arabian J. Chem.*, 2022, **15**, 104166.
25 M. Lorenzo Lopez, V. R. Kearns, J. M. Curran and E. A. Patterson, *Sci. Rep.*, 2024, **14**, 1–13.
26 B. Shriky, A. Kelly, M. Isreb, M. Babenko, N. Mahmoudi, S. Rogers, O. Shebanova, T. Snow and T. Gough, *J. Colloid Interface Sci.*, 2020, **565**, 119–130.
27 E. I. Taha, M. M. Badran, M. H. El-Anazi, M. A. Bayomi and I. M. El-Bagory, *J. Mol. Liq.*, 2014, **199**, 251–256.
28 S. Li, C. Yang, J. Li, C. Zhang, L. Zhu, Y. Song, Y. Guo, R. Wang, D. Gan, J. Shi, P. Ma, F. Gao and H. Su, *Int. J. Nanomed.*, 2023, **18**, 4485–4505.
29 P. Bergé and M. Dubois, *Contemp. Phys.*, 1984, **25**, 535–582.
30 A. Lupu, L. M. Gradinaru, D. Rusu and M. Bercea, *Gels*, 2023, **9**, DOI: 10.3390/gels9090719.
31 K. Y. Lee and D. J. Mooney, *Chem. Rev.*, 2001, **101**, 1869–1879.
32 R. Curvello, V. S. Raghuwanshi and G. Garnier, *Adv. Colloid Interface Sci.*, 2019, **267**, 47–61.
33 H. Cao, L. Duan, Y. Zhang, J. Cao and K. Zhang, *Signal Transduction Targeted Ther.*, 2021, **6**, DOI: 10.1038/s41392-021-00830-x.
34 L. Xuan, Y. Hou, L. Liang, J. Wu, K. Fan, L. Lian, J. Qiu, Y. Miao, H. Ravanbakhsh, M. Xu and G. Tang, *Nano-Micro Lett.*, 2024, 16, DOI: 10.1007/s40820-024-01421-5.
35 K. Joyner, S. Yang and G. A. Duncan, *APL Bioeng.*, 2020, **4**(4), DOI: 10.1063/5.0013707.
36 N. Bruot and H. Tanaka, *Phys. Rev. Res.*, 2019, **1**, 33200.
37 G. Romeo, A. Fernandez-Nieves, H. M. Wyss, D. Aciernoand and D. A. Weitz, *Adv. Mater.*, 2010, **22**, 3441–3445.
38 Q. Lian, K. Li, A. A. S. Sayyed, J. Cheng and J. Zhang, *J. Mater. Chem. A*, 2017, **5**, 14562–14574.
39 S. S. Thakur, S. K. Shenoy, J. S. Suk, J. S. Hanes and I. D. Rupenthal, *Eur. J. Pharm. Biopharm.*, 2020, **148**, 118–125.
40 J. Y. Tinevez, N. Perry, J. Schindelin, G. M. Hoopes, G. D. Reynolds, E. Laplantine, S. Y. Bednarek, S. L. Shorte and K. W. Eliceiri, *Methods*, 2017, **115**, 80–90.
41 D. K. Baby, *Rheology of hydrogels*, Elsevier Inc., 2019.
42 P. Calvert, *Adv. Mater.*, 2009, **21**, 743–756.
43 M. R. Islam and M. L. Oyen, *Mechanical characterization of hydrogels*, Elsevier Ltd, 2022, pp. 1-24..
44 E. M. Furst and T. M. Squires, *Microrheology*, Oxford Academic, Oxford, 2017, ch. 8, pp. 303–336..
45 E. M. Furst and T. M. Squires, *Microrheology*, Oxford Academic, Oxford, 2017, ch. 9, pp. 339–378..
46 T. De Li, H. C. Chiu, D. Ortiz-Young and E. Riedo, *Rev. Sci. Instrum.*, 2014, **85**, 12.
47 F. Giorgi, J. M. Curran and E. A. Patterson, *Sci. Rep.*, 2019, **9**, 1–6.